Published in final edited form as:
Int J Cancer. 2012 May 1; 130(9): 2176–2184. doi:10.1002/ijc.26251.

Boswellic Acid Inhibits Growth and Metastasis of Human Colorectal Cancer in Orthotopic Mouse Model By Downregulating Inflammatory, Proliferative, Invasive, and Angiogenic Biomarkers

Vivek R. Yadav[1], **Sahdeo Prasad**[1], **Bokyung Sung**[1], **Juri G. Gelovani**[2], **Sushovan Guha**[3], **Sunil Krishnan**[4], and **Bharat B. Aggarwal**[1,*]

[1]Department of Experimental Therapeutics, The University of Texas MD Anderson Cancer Center, Houston, Texas 77030, USA

[2]Department of Experimental Diagnostic Imaging, The University of Texas MD Anderson Cancer Center, Houston, Texas 77030, USA

[3]Department of Gastrointestinal Medicine and Nutrition, The University of Texas MD Anderson Cancer Center, Houston, Texas 77030, USA

[4]Department of Radiation Oncology, The University of Texas MD Anderson Cancer Center, Houston, Texas 77030, USA

Abstract

Numerous cancer therapeutics were originally identified from natural products used in traditional medicine. One such agent is acetyl-11-keto-beta-boswellic acid (AKBA), derived from the gum resin of the *Boswellia serrata* known as Salai guggal or Indian frankincense. Traditionally it has been used in Ayurvedic medicine to treat proinflammatory conditions. In the present report, we hypothesized that AKBA can affect the growth and metastasis of colorectal cancer (CRC) in orthotopically-implanted tumors in nude mice. We found that the oral administration of AKBA (50-200 mg/kg) dose-dependently inhibited the growth of CRC tumors in mice, resulting in decrease in tumor volumes than those seen in vehicle-treated mice without significant decreases in body weight. In addition, we observed that AKBA was highly effective in suppressing ascites and distant metastasis to the liver, lungs, and spleen in orthotopically-implanted tumors in nude mice. When examined for the mechanism, we found that markers of tumor proliferation index Ki-67 and the microvessel density CD31; were significantly downregulated by AKBA treatment. We also found that AKBA significantly suppressed NF-κB activation in the tumor tissue and expression of pro-inflammatory (COX2), tumor survival (bcl-2, bcl-xL, IAP-1, survivin), proliferative (cyclin D1), invasive (ICAM-1, MMP-9) and angiogenic (CXCR4 and VEGF) biomarkers. When examined for serum and tissue levels of AKBA, a dose-dependent increase in the levels of the drug was detected, indicating its bioavailability. Thus, our findings suggest that this boswellic acid analogue can inhibit the growth and metastasis of human CRC in vivo through downregulation of cancer-associated biomarkers.

Keywords

AKBA; colorectal cancer; NF-κB; growth; metastasis

*Corresponding author: Bharat B. Aggarwal, Phone: 713-794-1817; aggarwal@mdanderson.org.

Conflict of Interest Authors declare no conflicts of interest.

Introduction

Colorectal cancer (CRC) is the third most-common malignancy and the fourth most-frequent cause of cancer death in the United States. Lifestyle factors such as diet, exercise, and obesity have been linked to CRC risk. It seemed a bit broad to say it is primarily a disease of lifestyle [1]. Although surgical excision, chemotherapy, and radiotherapy are available, survival is still very poor when the disease is diagnosed at an advanced stage and better treatments are desperately needed. Thus, novel therapeutic agents, multitargeted to several mechanisms of carcinogenesis, are needed.

One increasingly promising source of therapeutic agents is traditional medicine from natural compounds. Numerous cancer therapeutics, including vincristine, vinblastine, camptothecin, doxorubicin, and paclitaxel, had their roots in plants thought to have medicinal value in traditional medicine. Several of these compounds have proved to be safe, effective, and multitargeted. One promising compound is boswellic acid, a pentacyclic triterpene derived from the fragrant gum resin of the bark of the *Boswellia serrata* tree. This resin is known as Salai guggul or Indian frankincense and is thought to be related to Biblical frankincense, which has been used for thousands of years for medicinal purposes. *Boswellia* has been used for centuries in traditional Ayurvedic medicine as a treatment for a wide variety of proinflammatory disorders. More recently, acetyl-11-keto-beta-boswellic acid (AKBA) has been tested in a number of such disorders, including rheumatoid arthritis [2], ulcerative colitis [3], and trinitrobenzene sulphonic acid-induced colitis in rats [4]. In humans, *Boswellia* extracts have been shown to exhibit activity against osteoarthritis [5], inflammatory bowel disease [6], chronic colitis [7], and collagenous colitis [8].

AKBA has been shown to inhibit leukotriene biosynthesis from endogenous arachidonic acid in intact peripheral mononuclear neutrophils through the inhibition of 5-lipooxygenase (LOX), yet has no effect on 12-LOX and cyclooxygenase (COX)-1 [9] observed. Boswellic acid can directly inhibit 5-LOX with a half maximal inhibitory concentration as low as 1.5 μM [10]. Other pentacyclic triterpenes (amyrin and ursolic acid) lack this effect on 5-LOX. Further studies have revealed that the pentacyclic triterpene ring structure, hydrophilic group on C4 ring A, and 11-keto function are all essential for this 5-LOX inhibitory activity [11]. It has been shown by photoaffinity labeling that AKBA binds to 5-LOX at a site distinct from its substrate binding site [12]. Unlike other pentacyclic triterpenes, boswellic acid inhibits the leukocyte elastase with a half maximal inhibitory concentration of 15 μM [13]. In addition to 5-LOX and elastase, AKBA was also found to bind and inhibit topoisomerase I and II α [14]. Its affinity constant for topo I and II α were 70.6 nM and 7.6 nM, respectively. Amazingly, this triterpene are “more potent inhibitors of human topoisomerases I and IIalpha than camptothecin, and amsacrine or etoposide, respectively.”

AKBA has been shown to inhibit the growth of a wide variety of tumor cells, including glioma [15], colon cancer [16, 17], leukemia [18-22], human melanoma [23], hepatocellular carcinoma [17], and prostate cancer [14]. Although AKBA can inhibit the growth of CRC cells [16, 17] and has shown activity against inflammatory bowel disease [6], whether it can inhibit the growth and metastasis of CRC in an orthotopic mouse model is not known. In the present report, we evaluated the activity of the orally administered boswellic acid analogue AKBA in a mouse xenograft model of human CRC. Our results indicate that AKBA is bioavailable and inhibits the growth and metastasis of human CRC *in vivo* through downregulation of inflammatory, proliferative, invasive, and angiogenic biomarkers.

Material and Methods

Materials

AKBA was kindly supplied by Sabinsa Corp (Piscataway, NJ). Polyclonal antibodies against intercellular adhesion molecule 1 (ICAM-1), cyclin D1, matrix metalloproteinase-9 (MMP-9), and IAP-1, and monoclonal antibodies against, Bcl-2, COX-2 and Bcl-xL were obtained from Santa Cruz Biotechnology (Santa Cruz, CA). Survivin was obtained from R&D system (Minneapolis, MN) and vascular endothelial growth factor (VEGF) was obtained from Thermo Fisher Scientific (Waltham, MA). Polyclonal antibodies against CXC receptor 4 (CXCR4) were obtained from Abcam (Cambridge, MA). The liquid DAB 1 substrate chromogen system with horseradish peroxidase that was used for immunocytochemical (IHC) analysis was obtained from DakoCytomation Ltd (Carpinteria, CA).

Animals

Male athymic nu/nu mice (4 weeks old) were obtained from the breeding colony of the Department of Experimental Radiation Oncology at The University of Texas MD Anderson Cancer Center (Houston, TX). The animals were housed 5 per cage in standard acrylic cages in a room maintained at constant temperature and humidity. Mice were housed under 12-h light and darkness cycles and were fed a regular autoclave chow diet with water ad libitum. Before initiating the experiment, we acclimatized all mice to a pulverized diet for 3 days. Mice were checked to ensure they were lesion-free and pathogen-free. Our experimental protocol was reviewed and approved by the Institutional Animal Care and Use Committee at MD Anderson Cancer Center.

Orthotopic human CRC mouse model

Human CRC cell line HCT116 was stably transfected with luciferase as previously described [24]. The luciferase-transfected HCT116 cells were then harvested from subconfluent cultures after brief exposures to 0.25% trypsin and 0.2% ethylenediaminetetraacetic acid. Trypsinization was stopped with a medium containing 10% fetal bovine serum. The cells were washed once in serum-free medium and resuspended in PBS. Only suspensions consisting of single cells with >90% viability were used for injections. Mice were anesthetized with a ketamine/xylazine solution, a small left abdominal flank incision was made, and 1.5×10^6 HCT116 cells suspended in 50 μL PBS were injected into each mouse's cecum using a 30-gauge needle and a calibrated push button-controlled dispensing device (Hamilton Syringe Company; Reno, NV). To prevent leakage, a cotton swab was held cautiously for 1 min over the injection site. The abdominal wound was closed in one layer with wound clips (Braintree Scientific, Braintree, MA).

Experimental protocol

One-and-a-half weeks after implantation, mice were randomly assigned to one of the following treatment groups (n = 6): (i) corn-oil vehicle only (100 μL daily) as the control; (ii) AKBA (50 mg/kg once daily, orally); (iii) AKBA (100 mg/kg once daily, orally); and (iv) AKBA (200 mg/kg once daily, orally by gavage) (Fig 1A). Tumor volumes were monitored weekly using the IVIS 200 bioluminescence imaging system and Living Image software (Caliper Life Sciences, Hopkinton, MA). Before imaging, animals were anesthetized in an acrylic chamber with a 2.5% isoflurane/air mixture and injected intraperitoneally with 40 mg/mL of D-luciferin potassium salts suspended in PBS at a dose of 150-mg/kg. After 10 min of incubation with the luciferin, mice were placed in a right lateral decubitus position and a digital gray-scale image was acquired, followed by the acquisition and overlay of a pseudocolor image representing the spatial distribution of

detected photons emerging from the active luciferase within the animal. Signal intensity was quantified as the sum of all detected photons within the region of interest per second per steradian.

Mice were imaged on days 0, 7, 14, 21, and 28 of treatment. Therapy was continued for 4 weeks and blood was collected by cardiac puncture after 2 h of AKBA treatment. Animals were sacrificed after 28 days. Blood plasma was separated and stored at -80°C. Primary tumors in the cecum were excised, and the final tumor volume was measured as $V= 2/3\ \pi r^3$, where r is the mean of the three dimensions (length, width, and depth). Metastatic colonies were counted in the liver, intestines, lungs, rectum, and spleen. The final tumor volume and the number of metastases were initially subjected to 1-way analysis of variance (ANOVA) and then later compared among groups using an unpaired Student t-test. Each excised tumor was divided into three parts. The first part of the tumor tissue was formalin-fixed and paraffin-embedded for routine hematoxylin-and-eosin staining and immunohistochemical (IHC) analysis. The second part was fixed in OCT for IHC analysis of Ki-67 and CD31. The third part was snap frozen in liquid nitrogen and stored at -80°C for archiving. Hematoxylin-and-eosin staining confirmed the presence of tumors in each cecum.

Measurement of NF-κB in CRC tissues

CRC tumor tissues (75–100 mg per mouse) from both control and experimental mice were minced and incubated on ice for 30 min in 0.5 mL of ice-cold buffer A consisting of 10 mM HEPES (pH 7.9), 1.5 mM KCl, 10 mM $MgCl_2$, 0.5 mM dithiothreitol, 0.1% IGEPAL CA-630 in the paragraph about materials. Also, please tell what the 0.1% was dissolved in.], and 0.5 mM phenylmethylsulfonyl fluoride. The minced tissue was homogenized using a dounce homogenizer and centrifuged at 16,000 *g* at 4°C for 10 min. The resulting nuclear pellets were suspended in 0.2 mL of buffer B consisting of 20 mM HEPES (pH 7.9), 25% glycerol, 1.5 mM $MgCl_2$, 420 mM NaCl, 0.5 mM dithiothreitol, 0.2 mM ethylenediaminetetraacetic acid, 0.5 mM phenylmethylsulfonyl fluoride, and 2-μg/mL leupeptin and were incubated on ice for 2 h with intermittent mixing. The suspension was then centrifuged at 16,000 *g* at 4°C for 30 min. The supernatant (nuclear extract) was collected and stored at -70°C until use. Protein concentration was measured by the Bradford protein assay with bovine serum albumin as the standard.

To assess NF-κB activation, we isolated nuclei from CRC tissue and carried out electrophoretic mobility shift assays as previously described [25]. In brief, nuclear extracts prepared from CRC tissue (as described in the previous step) were incubated with ^{32}P-end-labeled 45-mer double-stranded NF-κB oligonucleotides (4 μg of protein with 16 fmol of DNA) from the human immunodeficiency virus long-terminal repeat (5′-TTGTTACAA**GGGACTTTC CGCTG GGGACTTTC** CAGGGA GGCGT GG-3’ boldface indicates NF-κB binding sites) for 15 min at 37°C. The resulting DNA-protein complex was separated from free oligonucleotides on 6.6% native polyacrylamide gels. The dried gels were visualized, and radioactive bands were quantitated by a PhosphorImager (GE Healthcare, Sunnyvale, CA) using ImageQuant software.

Immunolocalization of VEGF, COX-2, MMP-9, and cyclin D1 in CRC tissues

The expression of VEGF, COX-2, MMP-9, and cyclin D1 were evaluated using an IHC method described previously [24]. In brief, CRC tumor samples were fixed with paraformaldehyde and embedded in paraffin. After being washed in PBS, the slides were blocked with protein block solution (DakoCytomation) for 20 min and incubated overnight with mouse monoclonal antihuman VEGF, COX-2, MMP-9, and cyclin D1 antibodies (1:100, 1:200, 1:100, and 1:200, respectively). Slides were washed and incubated with biotinylated link universal antiserum, followed by horseradish peroxidase-streptavidin

conjugate. The slides were rinsed and their color was developed using 3,3-diaminobenzidine hydrochloride as a chromogen. Finally, sections were rinsed in distilled water, counterstained with Mayer's hematoxylin solution, and mounted with DPX mounting medium for evaluation. Pictures were captured with a Photometrics CoolSnap CF color camera (Nikon, Lewisville, TX) and were analyzed with MetaMorph version 4.6.5 software (Universal Imaging; Downingtown, PA).

IHC analysis of Ki-67 in CRC tissues

Frozen sections (5 μm) were stained with anti-Ki-67 antibody (rabbit monoclonal clone SP6; NeoMarkers; Fremont, CA) as previously described [26]. Results were expressed as the percentage of Ki-67-positive cells ± the standard error per 40x magnification. Ten 40x magnification fields were examined and counted for each of three tumors from each treatment group. The values were initially analyzed using a 1-way ANOVA and then compared among groups using an unpaired Student t-test.

Microvessel density in CRC tissues

Ethanol-fixed, paraffin-embedded sections (5 μm) were stained with rat antimouse CD31 monoclonal antibodies (Pharmingen, San Diego, CA) as previously described [26]. Areas of highest microvessel density were then examined under high magnification (100x) and counted. Any distinct area of positive staining for CD31 was counted as a single vessel. Results were expressed as the mean number of vessels ± the standard error per high-power field (100x magnification). Twenty high-power fields were examined and counted for each of three tumors from each treatment group. The values were subjected to a 1-way ANOVA and then compared among groups using an unpaired Student t-test.

Western blot analysis of CRC biomarkers

Tumor tissues (75–100 mg per mouse) from control and experimental mice were minced and incubated on ice for 30 min in 0.5 mL of ice-cold whole-cell lysate buffer consisting of 10% NP-40, 5 M NaCl, 1 M HEPES, 0.1 M ethyleneglycoltetraacetic acid, 0.5 M ethylenediaminetetraacetic acid, 0.1 M phenylmethylsulfonyl fluoride, 0.2 sodium orthovanadate, 1 M NaF, 2 μg/mL aprotinin, and 2 μg/mL leupeptin. Minced tissue was homogenized using a dounce homogenizer and centrifuged at 16,000 *g* at 4°C for 10 min. Proteins were then fractionated by sodium dodecyl sulfate polyacrylamide gel electrophoresis, electrotransferred to nitrocellulose membranes, blotted with each antibody, and then detected by enhanced chemiluminescence (GE Healthcare, Piscataway, NJ).

Measurement of serum and tissue levels of AKBA

AKBA was determined by reverse-phase high performance liquid chromatography (HPLC) on a high-pressure chromatograph (Waters, Milford, Massachusetts) equipped with an ultraviolet detector and a 2.0 × 150-mm column (Gemini C18; particle size, 5 μm, 110A^0). The column was eluted in an isocratic flow with a component acetonitrile:methanol:acetic acid (1%) ratio of 70:20:10 at an eluent flow rate of 0.35 mL/min. The sample volume was 10 μL. The target compounds were detected at 250 nM. The solution components were identified and quantitatively analyzed using the external standard method with linear regression equations, reliability of approximation (R^2), and detection thresholds for AKBA by HPLC.

The pharmacokinetics of AKBA was studied in a treatment group of 24 mice that weighed 25-30 g. The AKBA was administered by mouth as a corn oil suspension in a dose of vehicle, 50, 100, or 200 mg/kg. The blood samples were taken from animals 3 h after the administration of AKBA or vehicle. The samples were centrifuged for 20 min at 2000 rpm

to obtain the blood plasma, treated with acetone (1.5:1) for deproteination, and centrifuged again for 15 min at 3000 rpm. The supernatant fraction was separated and extracted with chloroform (2:1). The chloroform extract was separated, the solvent was removed, and the dry residue was dissolved in methanol and analyzed by HPLC.

Statistical analysis

Statistical comparisons between drug-treated groups and the untreated control group were performed using 1-way ANOVAs. Data were presented as means ± standard deviations. *P* values of < 0.05 were considered statistically significant.

Results

The goal of our study was to determine whether AKBA can be used as a potential therapeutic agent against advanced CRC. To determine this, a nude mouse model with orthotopically transplanted human CRC was employed. The mechanisms by which AKBA manifests its effects were investigated in vivo at different dose concentrations. To facilitate tumor imaging in mice, luciferase-transfected human CRC cells were used.

AKBA inhibits growth of human CRC in mice

We used an orthotopically implanted human CRC xenograft nude mouse model to investigate the effects of AKBA on tumor growth. The protocol employed was outlined in Fig. 1A. We found a much more rapid increase in tumor volume in the vehicle group than in the three treatment groups. AKBA significantly suppressed tumor volume as determined by bioluminescence imaging *in vivo* (Fig. 1B) and by autopsy on the last day of the experiment using Vernier calipers (Fig. 1C). The tumor volume in the group receiving the highest dose of AKBA (200 mg/kg) was significantly lower than that in the control group on day 28 after treatment ($P < 0.001$ vs. vehicle) (Fig. 1B, *right panel*). In our present tumor inhibition model, the average tumor volume in the control mice increased from 2.49 ± 0.39 mm^3 to 8.91 ± 0.41 mm^3 after 28 days, whereas the average tumor volume in the AKBA-treated mice (200 mg/kg) decreased from 8.91 ± 0.41 mm^3 to 4.16 ± 0.19 mm^3, indicating that the proliferation rate of tumor cells in treated mice was greatly inhibited by AKBA. The results showed that AKBA 200 mg/kg ($P < 0.001$ vs. control) significantly decreased CRC growth; growth was further decreased in a dose-dependent manner ($P < 0.034$ vs. AKBA [100 mg/kg]; Fig. 1C, *left panel* and *right panel*). Additionally, there was no significant change in average animal weight between the control group and treated groups (Fig. 1D). Although we did not use survival as an endpoint, enhanced survival might have been expected in the treatment group.

AKBA inhibits distant organ metastasis and ascites in mice

Whether AKBA can inhibit the formation of ascites and distant organ metastasis was also investigated. We monitored the animals every day for ascites. Vehicle-treated mice developed ascites 21 days after tumor cell implantation, and this presence of ascites was confirmed at the time of sacrifice. AKBA significantly decreased the incidence of ascites in nude mice at 100 mg/kg, and at 200 mg/kg, the decrease was profound (Fig. 2A).

On day 35, mice were sacrificed and examined for the presence of metastasis. The results showed that CRC had metastasized to liver, lungs, and spleen in all control mice. However, AKBA inhibited metastasis to most organs when compared with the control vehicle (Fig. 2B).

AKBA downregulates proliferative and angiogenic biomarkers in CRC tissue

To determine how AKBA decreases CRC growth and metastasis, we first examined markers of proliferation and angiogenesis, Ki-67 and CD31, respectively. Our results showed that AKBA significantly decreased the expression of Ki-67 (Fig. 3A, *left panel*), and the largest decrease occurred at a dose of 200 mg/kg (Fig. 3A, *right panel*). AKBA also significantly decreased the expression of CD31, a marker of microvessel density (Fig. 3B, *left panel*), and again maximum decrease occurred at a dose of 200 mg/kg (Fig. 3B, *right panel*).

AKBA inhibits NF-κB activation in human CRC in mice

Because NF-κB has been linked to the growth and metastasis of CRC, we examined whether AKBA affects NF-κB activation in CRC tumor tissue. Electrophoretic mobility shift assay analysis for NF-κB in nuclear extracts from tumor samples showed that AKBA inhibited NF-κB activation in a dose-dependent manner. Maximum inhibition was found at a dose of 200 mg/kg (Fig. 4A).

AKBA downregulates the expression of inflammatory, survival, proliferative, invasive, and angiogenic proteins

NF-κB has been shown to regulate the expression of genes involved in inflammation, survival, proliferation, invasion, and angiogenesis [27]. Therefore, we evaluated the expression of these molecules in CRC tumor tissue from control and treated mice. A Western blot analysis revealed that AKBA decreased the expression of genes involved in inflammation (COX-2), proliferation (cyclin D1), invasion (MMP-9 and ICAM-1), angiogenesis (VEGF), and metastasis (CXCR4) (Fig. 4B). The expression of the antiapoptotic gene products Bcl-2, Bcl-xL, survivin, and IAP-1 was also downregulated at the dose of 200 mg/kg (Fig. 4B).

We also analyzed the expression of COX-2, VEGF, MMP-9, and cyclin D1 by IHC. We found that the expression of all these proteins was downregulated by AKBA in a dose-dependent manner in CRC tissue from orthotopically transplanted nude mice (Fig. 5A). These results were in agreement with those of the Western blot analysis.

Bioavailability of AKBA

Serum and CRC tissue levels of AKBA were examined by HPLC compared with pure AKBA (Fig. 6A). Serum levels of AKBA were determined 2 h after oral administration of 50, 100, or 200 mg/kg of the drug in mice (Fig. 6B). Levels of 138.8 ± 55.24, 477.6 ± 76, and 594.5 ± 40.36 ng/mL of the drug were detected at 50, 100, and 200 mg/kg doses, respectively. Levels in CRC tissues were 291.8 ± 14.4, 370.6 ± 3.6, and 405.0 ± 3.9 ng/g tissue at 50, 100, and 200 mg/kg doses, respectively (Fig. 6C). These results indicate that there is a strong correlation between tumor regression and the amount of AKBA in the blood plasma.

Discussion

CRC is one of the most lethal cancers, especially when it reaches the advanced stages. Because many cancer therapeutics have their roots in natural products, we investigated the effect of a boswellic acid analogue derived from a fragrant gum resin commonly used in Ayurvedic medicine for centuries. We investigated the effects of this triterpene on the growth and metastasis of CRC tumors in orthotopically transplanted nude mice. We found that AKBA alone suppressed the proliferation and metastasis of human CRC. This correlated with the downregulation of various biomarkers linked to inflammation, cell proliferation, cell survival, invasion, and angiogenesis (Fig. 5B).

We found that AKBA at 50 mg/kg significantly inhibited CRC growth in an orthotopic mouse model, but when the dose was increased to 200 mg/kg, it further enhanced the antitumor effects. This is the first report, to the best of our knowledge, wherein an orthotopic CRC model was applied to evaluate the preventive effects of oral administration of AKBA on CRC growth, metastasis, and CRC-induced ascites. More than 70% of tumor growth was inhibited by 200 mg/kg AKBA, and this level of inhibition was also seen in dose-dependent manner. The animals tolerated AKBA very well, as indicated by the lack of significant weight differences between treated and untreated mice from the start of the study.

The mechanisms by which AKBA acted *in vivo* were also investigated in detail. We found that oral administration of this triterpene decreases the levels of the proliferation marker Ki-67 and the microvessel density marker CD31. Additionally, the observed downregulation of various cell survival proteins and cyclin D1 may also contribute to the mechanism of action of AKBA against CRC. Numerous reports have suggested that cyclin D1 is closely associated with the proliferation of cancer cells [28]. Dai et al found that abnormal expression of cyclin D1 exists in CRC and may play an important role in its carcinogenesis [29]. Our findings suggested that AKBA downregulated cyclin D1 expression in CRC tumor tissues. Overexpression of COX-2 has been linked to the proliferation of CRC [30, 31]. The suppression of COX-2 expression by AKBA in CRC tissue may also account for its antitumor activity. We found that NF-κB in CRC tissue was downregulated in mice given AKBA compare with the controls. Since NF-κB activation has been linked with the growth of CRC, this may be another mechanism of action in this triterpene.

We found that the metastasis of CRC tumor to the lungs, liver, and spleen was also significantly suppressed by AKBA. The mechanism by which suppression of metastasis occurs was also investigated in detail. Although COX-2 expression has been associated with CRC metastasis [32], VEGF is the primary and most potent inducer of angiogenesis [33, 34]. VEGF activates cellular signaling pathways by binding to its receptor tyrosine kinase, which promotes several events required for angiogenesis, including endothelial cell survival, proliferation, and migration, and vascular permeability [35]. In the present study, AKBA downregulated the expression of VEGF in tumor tissues, indicating that it has antiangiogenic effects. Our results are in agreement with those of Pang et al, which suggested that AKBA inhibits prostate tumor growth by suppressing VEGF receptor 2-mediated angiogenesis in mice [36] We also found that AKBA downregulates CXCR4. The overexpression of CXCR4 and its role in CRC metastasis has been reported [37, 38]. Kim et al showed that CXCR4 expression in CRC patients increases the risk of recurrence, liver metastasis, and poor survival [39]. AKBA also suppressed the expression of the invasive gene *ICAM-1* in CRC tissue. AKBA inhibited metastasis-associated MMP-9 expression in CRC tumors as well [40]. This study suggested that AKBA suppressed the expression of various biomarkers important to the progression and metastasis of CRC tumors.

A very important aspect of an agent's ability to suppress tumors is the agent's bioavailability, which serves primarily a protective regulatory function constraining diffusion across capillaries in relation to lipid solubility and molecular weight. For a successful chemotherapeutic treatment, especially that involving tumor cell clusters invading adjacent tissues; the chemotherapy must be able to reach the blood. AKBA shows high lipid solubility [9], and we detected it in concentrations of up to 405 ng/gm in CRC tumors, which corresponded to concentrations of up to 494.5 ng/mL in the plasma at a dose of 200 mg/kg. The concentration of AKBA was a little higher in the plasma than in the CRC tissues. These results agree with those reported by Reising and colleagues [41] in a previous study of AKBA pharmacokinetics. Thus, these data demonstrate substantial levels of AKBA in CRC tumor tissue after a single oral dose and confirm the bioavailability of AKBA. These

results are further correlated with the tumor volume suppression and decrease in metastases to the lungs, liver, and spleen that we found with AKBA treatments.

Although our studies are the first to show the effect of AKBA against orthotopically implanted tumors, there are some reports about the chemopreventive effects of this agent against CRC. Previously, *Boswellia* extracts have been shown to be effective in animal models of chronic colonic inflammation-associated fibrosis in rats. Latella et al showed that 2,4,5-trinitrobenzene sulphonic acid-induced colitis in rats is prevented by oral administration of *Boswellia* extracts (50 mg/kg/day) [4]. Another study showed that AKBA can confer protection to mice with experimental ulcerative colitis induced by dextran sodium sulfate [3].

Boswellia extracts (350 mg thrice daily for 6 weeks) showed impressive effects in patients suffering from ulcerative colitis grades II and III [6] compared with controls treated with sulfasalazine (1 g thrice daily). All parameters tested improved after treatment with *Boswellia serrata* gum resin, with the results being similar to those of the controls: 82% of treated patients went into remission, as did 75% in the sulfasalazine group. Another study investigated the effects of AKBA in patients with chronic colitis [7]. Out of 20 patients treated with the agent, 18 showed an improvement in one or more study parameters; 14 went into remission compared to four of 10 in the sulfasalazine group. *Boswellia serrata* extracts have also been tested for the treatment of collagenous colitis in a double-blind, randomized, placebo-controlled, multicenter trial [8]. They concluded that *Boswellia serrata* extracts might be clinically effective in patients with collagenous colitis and suggested larger trials were needed to establish clinical efficacy.

Overall, our study showed that the natural compound AKBA acts as a promising agent against CRC tumors in vivo. In our xenograft mouse model, AKBA not only reduced tumor growth, but also suppressed distant metastasis and ascites, which strongly correlated with the inhibition of numerous biomarkers linked to inflammation, proliferation, invasion, angiogenesis, and metastasis.

Acknowledgments

We thank Walter P agel, Department of Scientific Publications for carefully editing the manuscript. Dr. Aggarwal is the Ransom Horne, Jr., Professor of Cancer Research. This work was supported by supported by a core grant (CA-16672), and a program project grant from National Institutes of Health (NIH CA-124787-01A2), and a grant from the Center for Targeted Therapy of MD Anderson Cancer Center.

References

1. Pearson JR, Gill CI, Rowland IR. Diet, fecal water, and colon cancer--development of a biomarker. Nutrition reviews. 2009; 67:509–26. [PubMed: 19703259]
2. Ammon HP. Salai Guggal - Boswellia serrata: from a herbal medicine to a non-redox inhibitor of leukotriene biosynthesis. European journal of medical research. 1996; 1:369–70. [PubMed: 9360935]
3. Anthoni C, Laukoetter MG, Rijcken E, Vowinkel T, Mennigen R, Muller S, Senninger N, Russell J, Jauch J, Bergmann J, Granger DN, Krieglstein CF. Mechanisms underlying the anti-inflammatory actions of boswellic acid derivatives in experimental colitis. American journal of physiology. 2006; 290:G1131–7. [PubMed: 16423918]
4. Latella G, Sferra R, Vetuschi A, Zanninelli G, D'Angelo A, Catitti V, Caprilli R, Gaudio E. Prevention of colonic fibrosis by Boswellia and Scutellaria extracts in rats with colitis induced by 2,4,5-trinitrobenzene sulphonic acid. European journal of clinical investigation. 2008; 38:410–20. [PubMed: 18489401]
5. Sengupta K, Alluri KV, Satish AR, Mishra S, Golakoti T, Sarma KV, Dey D, Raychaudhuri SP. A double blind, randomized, placebo controlled study of the efficacy and safety of 5-Loxin for

treatment of osteoarthritis of the knee. Arthritis research & therapy. 2008; 10:R85. [PubMed: 18667054]

6. Gupta I, Parihar A, Malhotra P, Singh GB, Ludtke R, Safayhi H, Ammon HP. Effects of Boswellia serrata gum resin in patients with ulcerative colitis. European journal of medical research. 1997; 2:37–43. [PubMed: 9049593]
7. Gupta I, Parihar A, Malhotra P, Gupta S, Ludtke R, Safayhi H, Ammon HP. Effects of gum resin of Boswellia serrata in patients with chronic colitis. Planta medica. 2001; 67:391–5. [PubMed: 11488449]
8. Madisch A, Miehlke S, Eichele O, Mrwa J, Bethke B, Kuhlisch E, Bastlein E, Wilhelms G, Morgner A, Wigginghaus B, Stolte M. Boswellia serrata extract for the treatment of collagenous colitis. A double-blind, randomized, placebo-controlled, multicenter trial. International journal of colorectal disease. 2007; 22:1445–51. [PubMed: 17764013]
9. Safayhi H, Mack T, Sabieraj J, Anazodo MI, Subramanian LR, Ammon HP. Boswellic acids: novel, specific, nonredox inhibitors of 5-lipoxygenase. The Journal of pharmacology and experimental therapeutics. 1992; 261:1143–6. [PubMed: 1602379]
10. Safayhi H, Sailer ER, Ammon HP. Mechanism of 5-lipoxygenase inhibition by acetyl-11-keto-beta-boswellic acid. Molecular pharmacology. 1995; 47:1212–6. [PubMed: 7603462]
11. Sailer ER, Subramanian LR, Rall B, Hoernlein RF, Ammon HP, Safayhi H. Acetyl-11-keto-beta-boswellic acid (AKBA): structure requirements for binding and 5-lipoxygenase inhibitory activity. British journal of pharmacology. 1996; 117:615–8. [PubMed: 8646405]
12. Sailer ER, Schweizer S, Boden SE, Ammon HP, Safayhi H. Characterization of an acetyl-11-keto-beta-boswellic acid and arachidonate-binding regulatory site of 5-lipoxygenase using photoaffinity labeling. European journal of biochemistry / FEBS. 1998; 256:364–8. [PubMed: 9760176]
13. Safayhi H, Rall B, Sailer ER, Ammon HP. Inhibition by boswellic acids of human leukocyte elastase. The Journal of pharmacology and experimental therapeutics. 1997; 281:460–3. [PubMed: 9103531]
14. Syrovets T, Buchele B, Gedig E, Slupsky JR, Simmet T. Acetyl-boswellic acids are novel catalytic inhibitors of human topoisomerases I and IIalpha. Molecular pharmacology. 2000; 58:71–81. [PubMed: 10860928]
15. Glaser T, Winter S, Groscurth P, Safayhi H, Sailer ER, Ammon HP, Schabet M, Weller M. Boswellic acids and malignant glioma: induction of apoptosis but no modulation of drug sensitivity. British journal of cancer. 1999; 80:756–65. [PubMed: 10360653]
16. Liu JJ, Duan RD. LY294002 enhances boswellic acid-induced apoptosis in colon cancer cells. Anticancer research. 2009; 29:2987–91. [PubMed: 19661305]
17. Liu JJ, Nilsson A, Oredsson S, Badmaev V, Duan RD. Keto- and acetyl-keto-boswellic acids inhibit proliferation and induce apoptosis in Hep G2 cells via a caspase-8 dependent pathway. International journal of molecular medicine. 2002; 10:501–5. [PubMed: 12239601]
18. Huang MT, Badmaev V, Ding Y, Liu Y, Xie JG, Ho CT. Anti-tumor and anti-carcinogenic activities of triterpenoid, beta-boswellic acid. BioFactors (Oxford, England). 2000; 13:225–30.
19. Shao Y, Ho CT, Chin CK, Badmaev V, Ma W, Huang MT. Inhibitory activity of boswellic acids from Boswellia serrata against human leukemia HL-60 cells in culture. Planta medica. 1998; 64:328–31. [PubMed: 9619114]
20. Hoernlein RF, Orlikowsky T, Zehrer C, Niethammer D, Sailer ER, Simmet T, Dannecker GE, Ammon HP. Acetyl-11-keto-beta-boswellic acid induces apoptosis in HL-60 and CCRF-CEM cells and inhibits topoisomerase I. The Journal of pharmacology and experimental therapeutics. 1999; 288:613–9. [PubMed: 9918566]
21. Xia L, Chen D, Han R, Fang Q, Waxman S, Jing Y. Boswellic acid acetate induces apoptosis through caspase-mediated pathways in myeloid leukemia cells. Molecular cancer therapeutics. 2005; 4:381–8. [PubMed: 15767547]
22. Bhushan S, Kumar A, Malik F, Andotra SS, Sethi VK, Kaur IP, Taneja SC, Qazi GN, Singh J. A triterpenediol from Boswellia serrata induces apoptosis through both the intrinsic and extrinsic apoptotic pathways in human leukemia HL-60 cells. Apoptosis. 2007; 12:1911–26. [PubMed: 17636381]

23. Zhao W, Entschladen F, Liu H, Niggemann B, Fang Q, Zaenker KS, Han R. Boswellic acid acetate induces differentiation and apoptosis in highly metastatic melanoma and fibrosarcoma cells. Cancer detection and prevention. 2003; 27:67–75. [PubMed: 12600419]
24. Kunnumakkara AB, Guha S, Krishnan S, Diagaradjane P, Gelovani J, Aggarwal BB. Curcumin potentiates antitumor activity of gemcitabine in an orthotopic model of pancreatic cancer through suppression of proliferation, angiogenesis, and inhibition of nuclear factor-kappaB-regulated gene products. Cancer research. 2007; 67:3853–61. [PubMed: 17440100]
25. Chaturvedi MM, Mukhopadhyay A, Aggarwal BB. Assay for redox-sensitive transcription factor. Methods in enzymology. 2000; 319:585–602. [PubMed: 10907546]
26. Guha S, Eibl G, Kisfalvi K, Fan RS, Burdick M, Reber H, Hines OJ, Strieter R, Rozengurt E. Broad-spectrum G protein-coupled receptor antagonist, [D-Arg1,D-Trp5,7,9,Leu11]SP: a dual inhibitor of growth and angiogenesis in pancreatic cancer. Cancer research. 2005; 65:2738–45. [PubMed: 15805273]
27. Aggarwal BB. Nuclear factor-kappaB: the enemy within. Cancer cell. 2004; 6:203–8. [PubMed: 15380510]
28. Mermelshtein A, Gerson A, Walfisch S, Delgado B, Shechter-Maor G, Delgado J, Fich A, Gheber L. Expression of D-type cyclins in colon cancer and in cell lines from colon carcinomas. British journal of cancer. 2005; 93:338–45. [PubMed: 16012517]
29. Dai WB, Ren ZP, Chen WL, Du J, Shi Z, Tang DY. Expression and significance of APC, beta-catenin, C-myc, and Cyclin D1 proteins in colorectal carcinoma. Ai zheng = Aizheng = Chinese journal of cancer. 2007; 26:963–6. [PubMed: 17927853]
30. Cho YB, Lee WY, Song SY, Shin HJ, Yun SH, Chun HK. Matrix metalloproteinase-9 activity is associated with poor prognosis in T3-T4 node-negative colorectal cancer. Human pathology. 2007; 38:1603–10. [PubMed: 17669467]
31. Sheng H, Shao J, Kirkland SC, Isakson P, Coffey RJ, Morrow J, Beauchamp RD, DuBois RN. Inhibition of human colon cancer cell growth by selective inhibition of cyclooxygenase-2. The Journal of clinical investigation. 1997; 99:2254–9. [PubMed: 9151799]
32. Tsujii M, Kawano S, DuBois RN. Cyclooxygenase-2 expression in human colon cancer cells increases metastatic potential. Proceedings of the National Academy of Sciences of the United States of America. 1997; 94:3336–40. [PubMed: 9096394]
33. Takakura, N. The Japanese journal of clinical hematology. Vol. 49. Rinsho ketsueki; 2008. Basic science of angiogenesis and its progress in clinical application; p. 1451-9.
34. Kowanetz M, Ferrara N. Vascular endothelial growth factor signaling pathways: therapeutic perspective. Clin Cancer Res. 2006; 12:5018–22. [PubMed: 16951216]
35. Ferrara N, Kerbel RS. Angiogenesis as a therapeutic target. Nature. 2005; 438:967–74. [PubMed: 16355214]
36. Pang X, Yi Z, Zhang X, Sung B, Qu W, Lian X, Aggarwal BB, Liu M. Acetyl-11-keto-beta-boswellic acid inhibits prostate tumor growth by suppressing vascular endothelial growth factor receptor 2-mediated angiogenesis. Cancer research. 2009; 69:5893–900. [PubMed: 19567671]
37. Tachibana K, Hirota S, Iizasa H, Yoshida H, Kawabata K, Kataoka Y, Kitamura Y, Matsushima K, Yoshida N, Nishikawa S, Kishimoto T, Nagasawa T. The chemokine receptor CXCR4 is essential for vascularization of the gastrointestinal tract. Nature. 1998; 393:591–4. [PubMed: 9634237]
38. Zeelenberg IS, Ruuls-Van Stalle L, Roos E. The chemokine receptor CXCR4 is required for outgrowth of colon carcinoma micrometastases. Cancer research. 2003; 63:3833–9. [PubMed: 12839981]
39. Kim J, Takeuchi H, Lam ST, Turner RR, Wang HJ, Kuo C, Foshag L, Bilchik AJ, Hoon DS. Chemokine receptor CXCR4 expression in colorectal cancer patients increases the risk for recurrence and for poor survival. J Clin Oncol. 2005; 23:2744–53. [PubMed: 15837989]
40. Xing LL, Wang ZN, Jiang L, Zhang Y, Xu YY, Li J, Luo Y, Zhang X. Matrix metalloproteinase-9-1562C>T polymorphism may increase the risk of lymphatic metastasis of colorectal cancer. World J Gastroenterol. 2007; 13:4626–9. [PubMed: 17729419]
41. Reising K, Meins J, Bastian B, Eckert G, Mueller WE, Schubert-Zsilavecz M, Abdel-Tawab M. Determination of boswellic acids in brain and plasma by high-performance liquid

chromatography/tandem mass spectrometry. Analytical chemistry. 2005; 77:6640–5. [PubMed: 16223251]

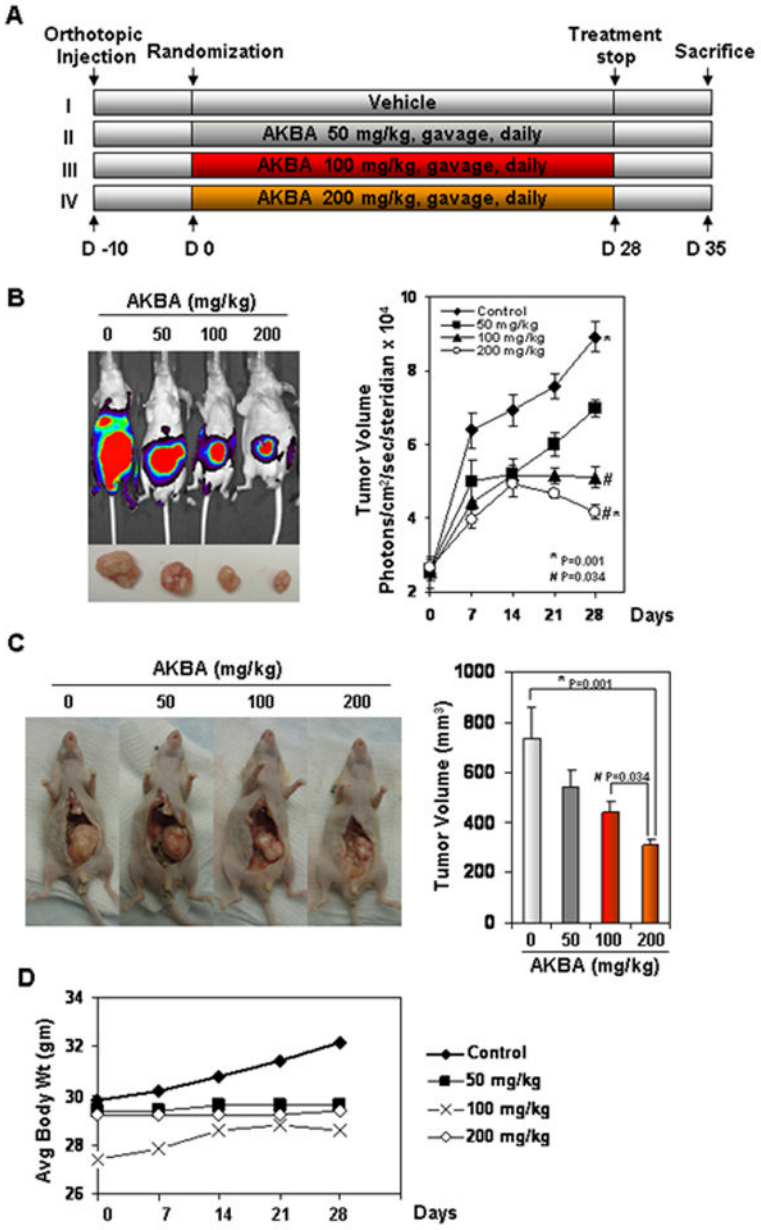

Figure 1.

AKBA inhibits the growth of orthotopically implanted CRC tumors in nude mice. (A) Schematic of the experimental protocol described in Materials and Methods. Group I was given corn oil (100 μL orally, daily); Group II was given AKBA (50 mg/kg orally, daily); Group III was given AKBA (100 mg/kg orally, daily); and Group IV was given AKBA (200 mg/kg orally, daily). (B) Bioluminescence imaging of orthotopically implanted CRC in live, anesthetized mice (left panel); measurements (photons/sec) of tumor volume (mean ± standard error) at various time points using live bioluminescence imaging at the indicated times (n = 6) (right panel). (C) Necropsy photographs of mice with orthotopically implanted CRC (left panel); tumor volumes (mean ± standard error; $P < 0.001$, control vs. 200-mg/kg AKBA and $P < 0.034$, control vs. 100-mg/kg AKBA) in mice measured on the last day of the experiment at autopsy using Vernier calipers and calculated using the formula $V = 2/3\ \pi r^3$ (n = 6). (D) As shown by the body weight change in mice, AKBA had no toxicity in the

amount tested. There was no significant difference in body weight between the treated group and the control group.

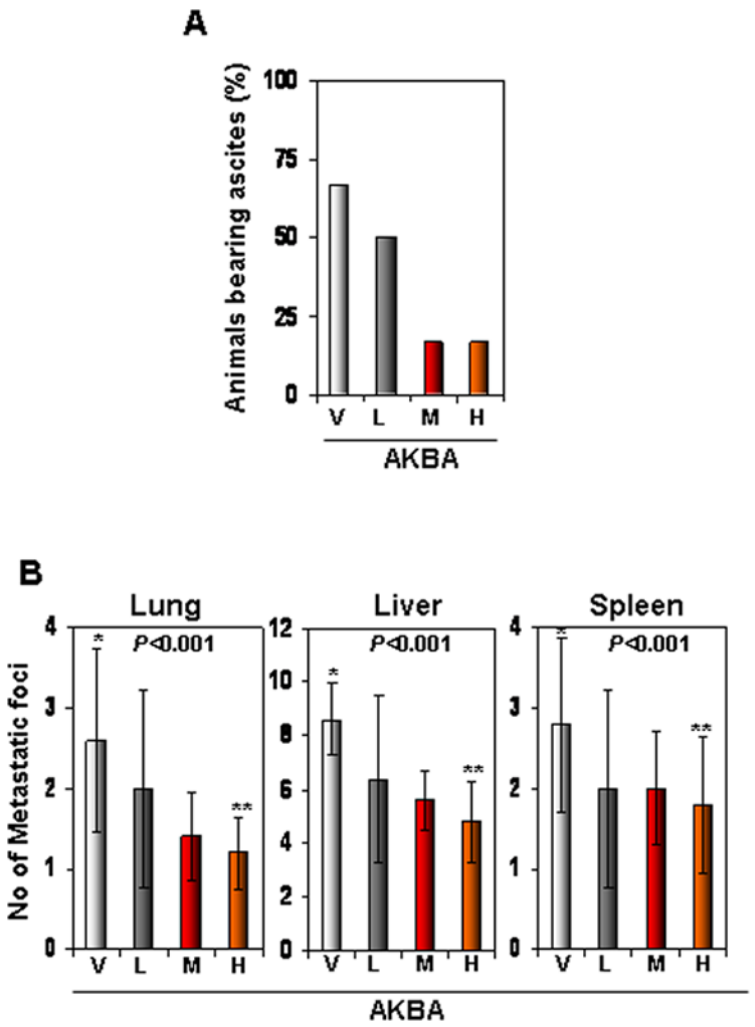

Figure 2.

AKBA inhibits ascites and distant organ metastasis in an orthotopic CRC murine model. (A) AKBA inhibited the development of ascites in CRC. The number of animals with ascites was counted 40 days after tumor cell implantation, and the percentages of animals with ascites were plotted. V, vehicle; L, low (AKBA 50 mg/kg); M, medium (100 mg/kg); and H, high (200 mg/kg). (B) AKBA inhibited metastasis to the lungs, liver, and spleen. Mice were killed and their abdomens were surgically opened; the number of metastatic foci in each organ was counted. Values are the mean ± standard deviation, n = 6. V, vehicle; L, low (AKBA 50 mg/kg); M, medium (100 mg/kg); and H, high (200 mg/kg).

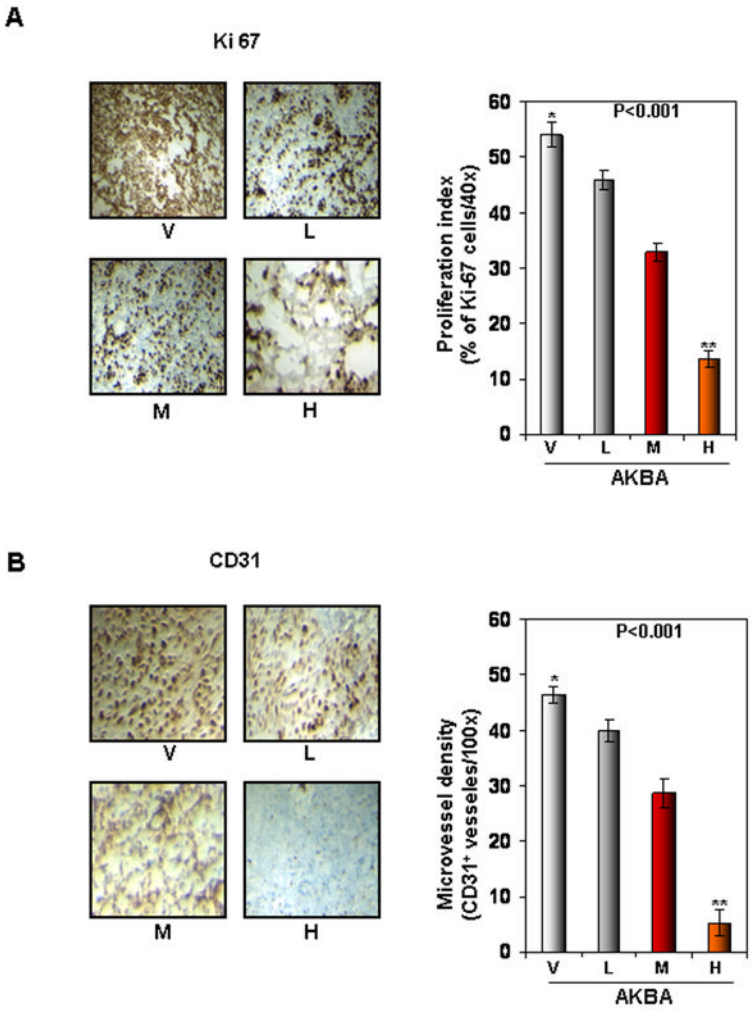

Figure 3.

AKBA inhibits tumor cell proliferation and angiogenesis in CRC. (A) The results of an IHC analysis of proliferation marker Ki-67 indicated that CRC cell proliferation was inhibited in mice treated with AKBA at different dose concentrations: V, vehicle; L, low (AKBA 50 mg/kg); M, medium (100 mg/kg); and H, high (200 mg/kg) (*Left panel*). Quantification of Ki-67 cells, as described in Materials and Methods. Values are represented as the mean ± standard error of triplicate (*Right panel*). (B) The results of an IHC analysis of CD31 for microvessel density indicated that angiogenesis was inhibited by AKBA at different dose concentrations. V, vehicle; L, low (AKBA 50 mg/kg); M, medium (100 mg/kg); and H, high (200 mg/kg) (*Left panel*). Quantification of CD31-positive microvessel density, as described in Materials and Methods. Values are the mean ± standard error of triplicate.

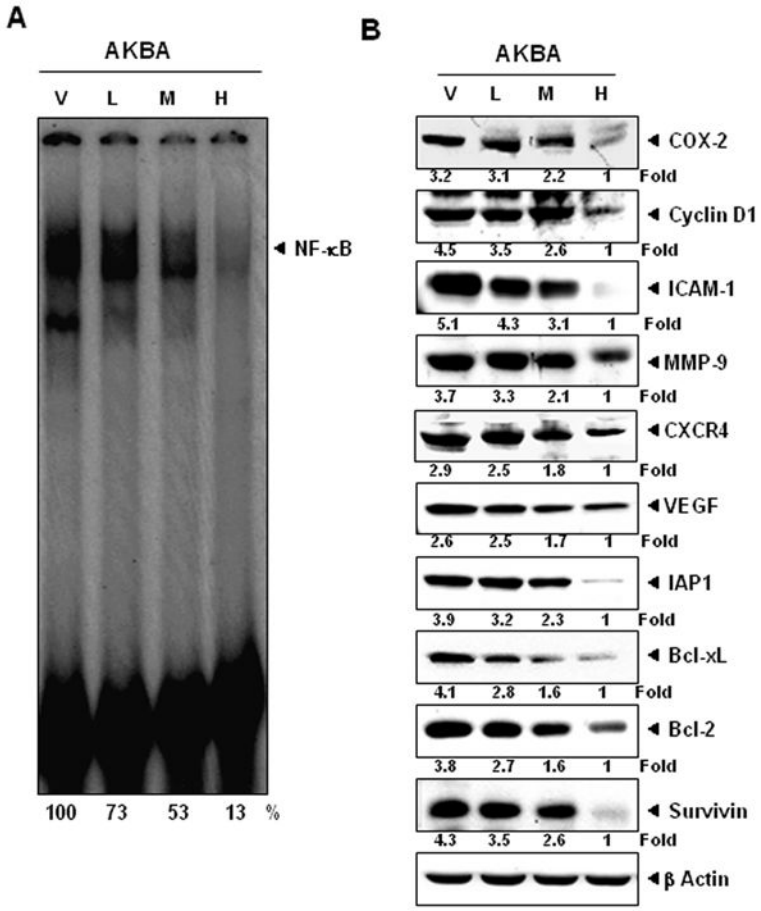

Figure 4.

AKBA inhibits the expression of NF-κB and NF-κB-regulated gene products in CRC samples. (A) Electrophoretic mobility shift assay analysis showed the inhibition of NF-κB by AKBA in nuclear extracts from animal tissue. (B) Western blot showing that AKBA inhibited the expression of NF-κB-dependent gene products that regulate proliferation (cyclin D1 and COX-2), invasion (ICAM-1 and MMP-9), metastasis (CXCR4), and angiogenesis (VEGF). AKBA inhibits the expression of antiapoptotic gene products such as IAP-1, Bcl-xL, Bcl-2, and survivin in CRC tissues. Samples from three animals in each group were analyzed, and representative data are shown. V, vehicle; L, low (AKBA 50 mg/kg); M, medium (100 mg/kg); and H, high (200 mg/kg).

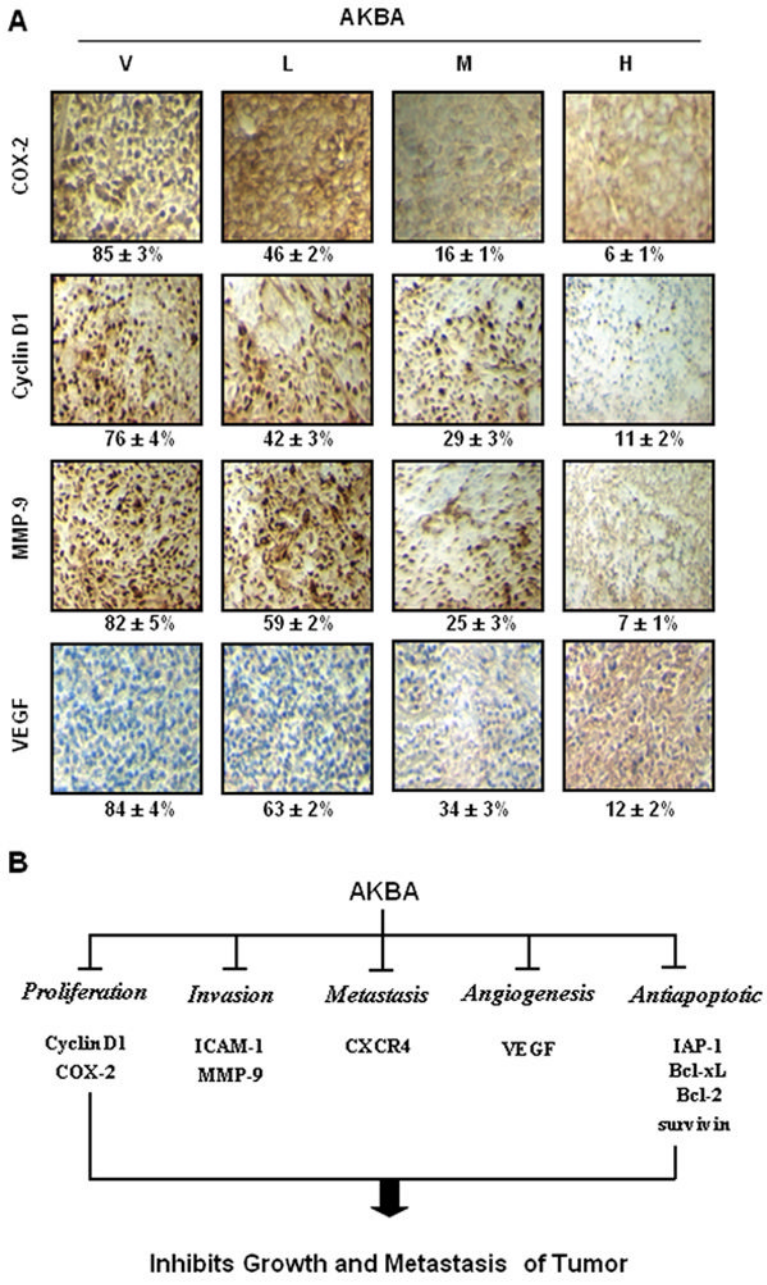

Figure 5.

(A) AKBA inhibits the expression of COX-2, cyclin D1, MMP-9, and VEGF in CRC tissues from mice. Percentages indicate positive staining for the given biomarker. Samples from three animals in each group were analyzed, and representative data are shown. V, vehicle; L, low (AKBA 50 mg/kg); M, medium (100 mg/kg); and H, high (200 mg/kg). (B) Schematic representation of mechanism by which AKBA inhibited growth/ Metastasis of orthotopically implanted CRC.

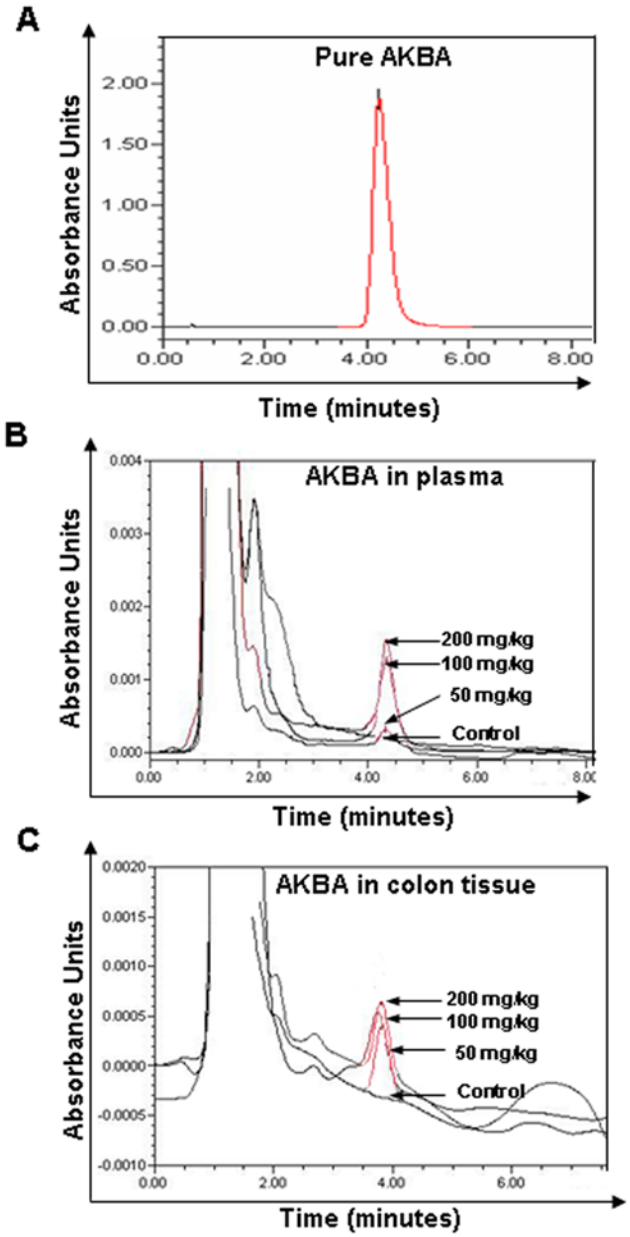

Figure 6.

HPLC chromatogram of AKBA in plasma and CRC tissue in nude mice. (A) HPLC chromatogram of pure AKBA. (B) HPLC chromatogram of AKBA in mice plasma from dosed animal, n = 6. (C) HPLC chromatogram of AKBA in mice CRC tissue from dosed animal, n = 6.